AAPS PharmSciTech (2019) 20: 94
DOI: 10.1208/s12249-019-1302-6

Research Article

Theme: Paul Myrdal Memorial Issue - Pharmaceutical Formulation and Aerosol Sciences
Guest Editors: Philip J. Kuehl and Stephen W. Stein

Assessing Aerosol Performance of a Dry Powder Carrier Formulation with Increasing Doses Using a Novel Inhaler

Stewart Yeung,[1] Daniela Traini,[1] Alan Tweedie,[2] David Lewis,[2] Tanya Church,[2] and Paul M. Young[1,3,4]

Received 9 October 2018; accepted 3 January 2019; published online 28 January 2019

Abstract. This study aims to investigate the implications of loaded formulation mass on aerosol performance using a reservoir novel dry powder inhaler containing a custom dosing cup to deliver carrier-based formulation to the lungs. A 3D printed dosing cup with volume size of 133.04 mm^3 was manufactured to allow for the progressive loading of different carrier formulation masses of 1% beclomethasone dipropionate BDP (*w*/*w*) formulation (10 to 60 mg, with increments of 10 mg), in a novel customizable DPI device. Scanning electron micrographs were used to investigate BDP detachment from carrier particles post-aerosolisation and particle deposition on the USP induction port. The subsequent aerosol performance analysis was performed using the next generation impactor (NGI). Incrementally increasing the loading mass to 60 mg led to decreases in BDP detachment from carrier particles, resulting in significant decreases in aerosol performance. Increases in loading dose mass led to progressively decreased detachment of BDP from the carrier and the overall aerosol performance in comparison to the initial mass of 10 mg. These results are likely to be due to a decrease in void volume within the dosing cup with increased loading mass leading to altered airflow, decreased impaction forces and the possibility of a significant quantity of large carrier particles introducing a 'sweeping' effect on the inhaler inner surface. This study has shown that despite the decreased BDP detachment from the carrier and decreased aerosol performance, the dose delivered to the lung still increased due to the higher loaded dose.

KEY WORDS: novel dry powder inhaler; loading dose; carrier formulation; dispersion forces; aerosol performance.

INTRODUCTION

The conventional use of dry-powder inhalers (DPI) for conditions such as asthma and chronic obstructive pulmonary disease tends to be by delivering relatively low drug doses to the lungs (1,2). Still, increasingly, DPIs are being utilised to deliver greater amounts of active pharmaceutical ingredients (API) to the lungs such as colistimethate sodium (Colobreathe®) and tobramycin (TOBI®) for cystic fibrosis, and laninamivir (Inavir®) for the prophylaxis of influenza A and B (3–6). Generally, to increase the amount of API delivery to the lungs, an increase in API percentage (weight/weight) within the formulation and/or increasing the loading dose quantity of the formulation to deliver the desired quantity to the lungs is required.

However, by increasing the concentration of API, reformulation is needed since greater inter-particular forces can arise, with subsequent particle agglomeration and decrease in aerosol performance (2,7). By increasing the formulation loading mass, it is potentially possible to increase API delivery to the lungs, without reformulating into a high concentration API containing dry powder. However, increasing the loading dose of a typical reservoir-type inhaler necessitates the optimisation of existing DPI devices or the designing of a novel inhaler, enabling the sufficient loading of greater mass and the dispersion of the dry powder formulation.

There are only a limited number of dry powder inhaler devices currently available on the market with large loading masses (Podhaler®, Turbospin®, Twincaps® and Diskhaler®) delivering a variety of API. However, a number of large loading mass DPIs (both conventional and specifically engineered for high masses) have also been investigated to deliver large amounts drug to the lungs, with varying aerosol performances (Table I). The dry-powder inhalers vary

[1] Respiratory Technology, the Woolcock Institute for Medical Research and Discipline of Pharmacology, Faculty of Medicine and Health, University of Sydney, Sydney, NSW 2006, Australia.
[2] Chiesi Limited, Chippenham, Wiltshire, UK.
[3] 431 Glebe Point Road, Glebe, NSW 2037, Australia.
[4] To whom correspondence should be addressed. (e–mail: paul.young@sydney.edu.au)

in type and design; capsule based (*e.g.* maximum 125-mg loading dose in the Turbospin®), blister or unit dose devices based with pre-measured individual dosing units (*e.g.* maximum 12.7-mg loading dose in the Incruse Ellipta®), reservoir-based (maximum of 10.1-mg loading dose in the NEXThaler®) and also the Orbital® which contains a puck (dosing compartment) that can hold a dose up to 400 mg of formulation (12,15,19,20). These high mass DPIs are passive inhalers, with variable maximal aerosol performances dependent on the type of formulation used and the design of the inhaler. Previous studies have shown that optimisation of existing DPIs to increase the amount of dry powder loading is possible with modification and optimisation of the inhaler device without being detrimental to the aerosol performance (8,10). Currently, there is no high-dose formulation (carrier based) that utilises a reservoir-based device neither on the market nor, to our knowledge, any current investigations ongoing in this field.

This investigation aims to examine the impact of increasing formulation loaded mass in a novel reservoir-based inhaler on particle dispersion, aerosol performance and resultant *in-vitro* API delivery, using a conventional carrier-based formulation. Computer-aided design and 3D printing of enlarged sized dosing cup within the novel DPI were investigated, thus enabling the progressive increased loading. This allowed for a better understanding of aerosol dispersion with increasing formulation loaded mass that was independent of formulation composition.

MATERIALS AND METHODS

Materials

Micronised beclomethasone dipropionate (BDP), coarse granular α-lactose monohydrate (sieve fraction of 212–355 μm) as carrier particle, micronised α-lactose monohydrate and magnesium stearate as pre-blend were supplied by Chiesi Ltd. (Chippenham, United Kingdom). Deionised water, used throughout this study, was purified by reverse osmosis (MilliQ, MilliPore, Australia). All chemicals used were of high-performance liquid chromatography (HPLC) analytical grade and purchased from Chem-Supply (South Australia, Australia).

Novel Dry Powder Inhaler 'Rig' Device

A novel customizable dry powder inhaler device rig was used to test the *in vitro* aerosolisation performance of the carrier-based formulation. The rig used for this study consisted of a single dose, manually fed, dosing cup with four components: (1) base with dosing cup, (2) cyclone chamber, (3) cyclone inlet with chimney outlet and (4) mouthpiece

Table I. Example of Investigations into High Mass Loading Inhaler Devices on Aerosol Performance

Device	Type	Formulation type	Maximum fill mass (mg)	Maximum FPF (< 5 μm*)	Ref.
Aerolizer®	Capsule	Spray-dried rifapentine Spray-dried colistin Spray-dried tobramycin	30 mg 50 mg 100 mg	66.1 ± 2.4% (FPF recovered) 61.8 ± 3.2% (FPF recovered) 62.7 ± 1.5% (FPF recovered)	(8)
CC_{90}-3D	Capsule	Excipient enhanced growth-ciprofloxacin formulation	25 mg	94.8 ± 0.4% (FPF emitted)	(9)
Cyclops	Disposable multiple air classifier	Spray-dried tobramycin	30 mg + 20 mg lactose as sweeper crystals	90.7% (FPF delivered)	(10)
Diskhaler®	Blister	Zanamivir carrier formulation	25 mg	34.2 ± 0.9% (FPF loaded)	(11)
Fluidised-bed (FB)-DPI	Dosing sphere	Excipient enhanced growth-ciprofloxacin formulation	100 mg	93.3 ± 0.3% (FPF emitted)	(9)
Orbital®	Puck (sample compartment)	Co-sprayed tobramycin and mannitol	400 mg	38.8 ± 2% (FPF loaded ≤ 6.8 μm)	(12)
Podhaler®	Capsule	Spray-dried tobramycin PulmoSpheres®	50 mg	68.8 ± 2.10% (FPF emitted < 6.8 μm)	(4,13,14)
Turbospin®	Capsule	Micronised colistimethate sodium	125 mg	20.2% (FPF emitted)	(15,16)
Twincaps® (scaled up)	Single-unit disposable	Spray-dried amorphous composite particles	80 mg	54.9% (FPF emitted)	(17)
Twincer™	Disposable multiple air classifier	Micronised colistimethate sodium	50 mg	59.4% (57.4–62.4) (FPF real dose)	(18)
Twinmax™	Single-unit disposable	Spray-dried, API-only formulation of a novel synthetic protein, AP301	100 mg	30.0% (FPF loaded)	(17)

*FPF for particles sized < 5 μm unless otherwise specified
FPF emitted, fine particle fraction of emitted dose; FPF emitted < 6.8 μm, fine particle fraction of emitted dose with particles sized < 6.8 μm; FPF delivered, fine particle fraction of delivered dose; FPF loaded, fine particle fraction of loaded dose; FPF loaded ≤ 6.8 μm, fine particle fraction of dose loaded with particles sized ≤ 6.8 μm; FPF real dose, fine particle fraction of the precise amount of drug weighed into the blister; FPF recovered, fine particle fraction of recovered dose

secured together by four stainless steel screws (Fig. 1). A large 3D printed dosing cup of 133.04mm^3 was manufactured to allow increased mass loading for the focus of this study; previous studies utilised a standard 16.26-mm^3 cup similar to that of the NEXThaler® inhaler (2). Also, the internal geometry of the rig inhaler (absence of the breath-actuated mechanism) is similar to that of the NEXThaler® which has an inspiratory flow resistance of 0.036 kPa$^{1/2}$ L/min corresponding to a flow rate of 55 L/min at 4 kPa (21). Components of the rig were prepared using a 3D printer (Objet30 Pro, Stratasys Eden Prairie, MN, USA) using VeroClear (all components except base with dosing cup) and VeroBlack Plus (base with dosing cup) plastics (Stratasys Eden Prairie, MN, USA), with layering thickness of 16 μm for VeroClear and 28 μm for VeroBlack Plus, respectively; both had an overall build accuracy of 0.1 mm.

Formulation Preparation

The BDP-carrier formulation was prepared in three sequential steps. Initially, coarse granular α-lactose monohydrate was mixed with pre-blend at a ratio of 9:1 *w*/*w* (135-g lactose to 15-g pre-blend) in a glass container (700-mL volume) using a commercial low shear 3-dimensional shaker-mixer (Alphie-03, Hexagon Product Development PVT. LTD., Vadodara, India) for 4 h at 32 rpm. The resulting carrier formulation was rested for further 24 h to allow for electrostatic discharge, prior to preparing the formulations containing the BDP.

The analysed formulation used in this study contained 1% (*w*/*w*) BDP with 89.1% coarse lactose carrier and 9.9% of pre-blend. The BDP (0.1 g) together with the pre-blend carrier system (9.9 g) was mixed in a plastic container (50-mL volume) using the shaker mixer for 90 min at 32 rpm. A 400-μm mesh was then used to sieve the resultant powder formulation to break up large agglomerates that may have formed and returned to the mixer for a further 30 min at 32 rpm. The formulation was allowed to rest for a further 24 h before being investigated. Formulations were stored at 10% relative humidity and tested at 33.5 ± 7.2% relative humidity.

Physical Characterisation

Scanning Electron Microscopy

The particle morphology of the formulation together with particles collected in the USP induction port and pre-separator of the NGI post-aerosolisation were analysed. To capture post-aerosolisation particles, circular carbon tape (double-sided adhesive) was attached and positioned on the inner inlet surface of the USP induction port. Also, for the pre-separator, a stub (viewing stub used for SEMs) attached with circular carbon tape was placed in the dry well. Particles were evaluated using scanning electron microscopy (SEM JCM-6000 Neoscope Scanning Electron Microscope, Joel Ltd., Akishima Tokyo, Japan). The formulation particles and post-aerosolisation particles were prepared in the same manner for imaging. The SEM was operated at an accelerat-

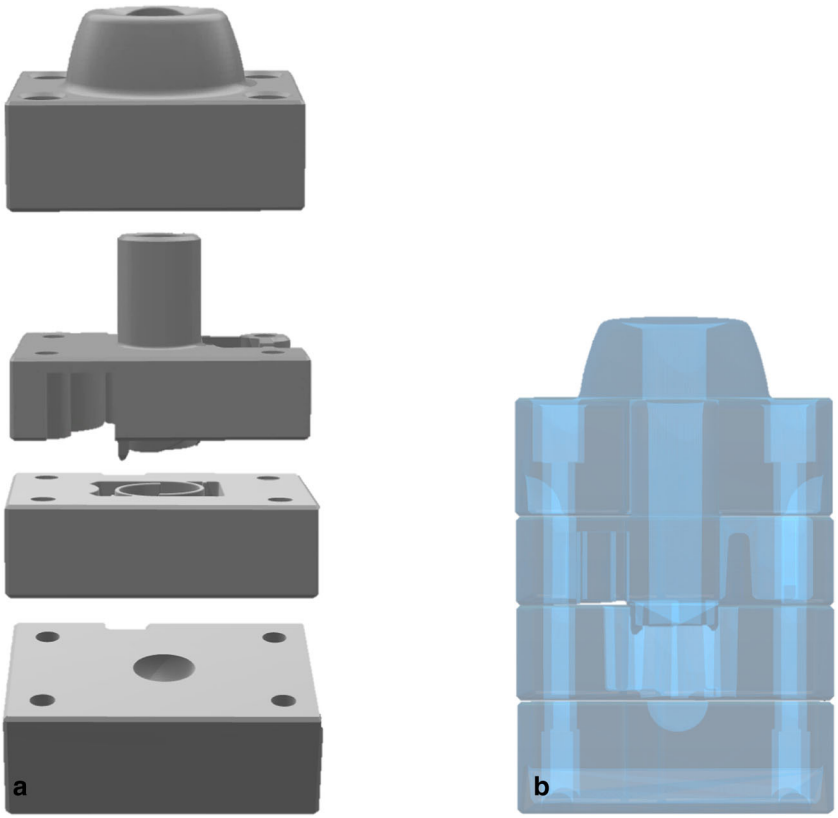

Fig. 1. **a** Unassembled novel dry powder inhaler 'Rig' consisting of four 3D printed parts with novel large dosing cup (133.04mm^3) and **b** X-ray view of assembled Rig (viewed in 3D Builder, Microsoft Corporation)

ing voltage of 10-15 kV, with samples prepared by positioning on circular carbon tape, attached atop of a viewing stub and coated with 15 nm thickness of gold using a sputter coater (Smart Coater, Joel Ltd., Akishima Tokyo, Japan).

Bulk Density

The bulk density of the formulation was obtained using the untapped powder density method. In brief, sufficient amount of formulation was incrementally added to the 4-mL volume index of a 10-mL measuring cylinder and resultant net weight noted. The resultant net weight was divided by the 4-mL volume of the measured filled to calculate the resultant bulk density and expressed as milligram per cubic millimetre. The formulation was analysed in triplicate.

Drug Content Uniformity

The drug content uniformity was analysed after the preparation of the formulation as outlined in the British Pharmacopoeia Volume V Appendix XII C. 3. Test B (22). In brief, the formulation was evenly dispersed over wax paper and ten random samples assayed by placing 15 ± 1 mg in individual 50-mL volumetric flasks, which were subsequently made up to volume with HPLC grade methanol and water (80:20% *v*/*v*), filtered with a 0.22-μm nylon filter and chemically assayed by HPLC. The resultant BDP concentration for each sample was conveyed as a percentage compared to that of the theoretical calculated amount in the sample dose. As per requirement by the pharmacopoeia, each sample has to be in the range of 85–115% of the nominal dose.

Chemical Analysis with High-Performance Liquid Chromatography

An HPLC system equipped with an SPD-20A UV-VIS detector, LC-20AD solvent delivery unit and SIL-20A HT auto-sampler (Shimadzu, Kyoto, Japan) was used to analyse the BDP content of each sample. A Luna C-18 column (150 × 4.6 mm, 3 μm, Phenomenex, Torrance, USA) was used with isocratic flow of 1 mL/min de-gassed. Filtered (nylon 0.45 μm, GVS life sciences, Sanford, USA) and sonicated (5 min) mobile phase containing methanol:water (80:20% *v*/*v*) was used for analysis. For the detection of BDP, a wavelength of 243 nm was used. Calibration curves between concentrations of 0.5 μg/mL and 100 μg/mL was prepared using the mobile phase for determining BDP concentration of each sample. The injection volume was 100 μL and retention time of 5.85 ± 0.14 s. The limit of detection was 0.32 μg/mL.

Evaluation of In Vitro Drug Deposition and Aerosol Performance

The aerosol performance of various loading doses of formulation was assessed using the NGI. The flow rate was set at 60 L/min calibrated using a mass flow meter (Model 4040, TSI Incorporated, Shoreview, Minnesota, USA) for 4 s using a vacuum pump (Model WP, Westech, Bedfordshire, UK) equipped with a critical flow controller (Model TPK2000, Copley, Nottingham, UK). The NGI collection plates (Stages 1–7 and micro-orifice collector) were thinly coated with a lubricant spray (Specialist high performance silicone, WD-40, California, USA) to prevent particle bounce and the reintroduction of fine particles back into airflow. Each delivered actuation from the rig device contained 10, 20, 30, 40, 50 and 60 ± 1 mg of formulation loaded into the disassembled rig-dosing cup. For each loading mass, the number of actuations from the device was dependent on the overall BDP content in the loading massed tested to ensure accurate and precise HPLC results, but not exceeding 10 actuations as outlined by British Pharmacopoeia (23). Specifically, 10 actuations were used for loading masses of 10 mg, 5 actuations with loading masses of 20 mg, 3 actuations for with loading masses of 30 mg, 2 actuations with loading masses of 40 mg, 2 actuations with loading masses of 50 mg and 2 actuations with loading masses of 60 mg, respectively.

After the final actuation, the device and all stages of the impactor were washed and diluted with mobile phase of specific volumes: rig inhaler device 10 mL; rig/USP induction port adapter 5 mL; USP induction port 10 mL; pre-separator 50 mL; stage 1 and micro-orifice collector (MOC) 10 mL and stages 2–7 5 mL. All samples were filtered with 0.22-μm nylon filter and quantified for BDP using HPLC. As per requirement by the British Pharmacopoeia, the total mass recovered required to be in the range of 85–115% of the nominal dose. Each formulation was analysed in triplicate.

The combined mass of recovered BDP obtained from HPLC results for the rig device and all stages of the NGI were analysed to obtain log-normal probability plots, cumulative particle percentage *versus* log stage particle size effective cutoff diameters at the test flow rate of 60 L/min (stages 1 to MOC 8.06, 4.46, 2.82, 1.66, 0.94, 0.55, 0.34 and 0.00 μm, respectively). With these results, the emitted fine particle fraction (FPF emitted %, percentage of particles ≤ 5 μm of the emitted dose), total dose fine particle fraction (FPF total dose %, percentage of particles ≤ 5 μm of the total dose), fine particle dose (FPD, mass of particles ≤ 5 μm), aerodynamic particle size parameters, mass median aerodynamic diameter (MMAD, calculated as the 50th percentage particle size distribution) and geometric standard deviation (GSD, calculated as the square root of 84.13th/15.87th percentile) was subsequently calculated. These aerosol performance and aerodynamic particle size parameters were calculated with the use of Copley Inhaler Testing Data Analysis Software (CITDAS) (Version 3.10 Wibu, Copley, Nottingham, UK).

Statistical Analysis

Statistical analysis was applied using two-tailed *t* tests, assuming unequal variance with $n = 3$. Results were expressed as the mean and standard deviation (SD). Statistical differences were determined and concluded as significant with p value of less than 0.05.

RESULTS AND DISCUSSIONS

Scanning Electron Microscopy

Scanning electron micrographs were taken of coarse granular lactose carrier, pre-blend carrier system and pre-blend carrier system containing the 1% (*w*/*w*) BDP formulation (Fig. 2). It was observed that the coarse granular lactose carrier presented a rough surface, with considerable sized crevices, also known as active sites, which are high-energy

binding sites dominating the surface (24). Studies have shown that greater energy is required to detach fine particles (*i.e.* API) from these crevices, as opposed to particles attached onto the smooth surface of the carrier (25–27). This study employed a lactose carrier pre-treated with micronised α-lactose monohydrate and magnesium stearate (a pre-blend) to occupy these crevices, as per previous study (2). This pre-treated lactose carrier is known as pre-blend carrier and enabled the BDP to attach onto the newly formed smoother surface, preventing BDP to be trapped in the active sites, allowing the BDP to detach from the lactose carrier with greater efficiency at the same airflow velocities and turbulent/impaction forces induced by the inspiratory air flow.

Influence of Dose Loading on Post-Aerosolisation USP Induction Port Deposition and Carrier Surface Morphology

Micrographs of particles deposited on the surface of the USP induction port post-aerosolisation were evaluated. In general, a sparse distribution of fine particles was observed when the 10-mg formulation loading was delivered (Fig. 3a). Furthermore, with the 20-mg and 30-mg dose loading, greater proportions of dry powder are being aerosolised compared to that of the 10 mg. This results in greater number of fine particle deposition onto the inner surface of the USP induction port, with increases of ~ 24% and ~ 73%, respectively (Fig. 3b, c). It is also interesting to note that not only a greater number of particles deposited on the surface of the USP induction port for loading doses from 40 to 60 mg with ~ 55%, ~ 56% and ~ 102%, but particles are visually larger in size (Fig. 3d–f). For the loading dose of 60 mg, closely clustered fine particles could also be distinguished, possibly indicating carrier particles attached with BDP fine particles contacting the induction port surface (Fig. 3f). However, fine particles can be seen attached to the relative larger particles in the 40-, 50- and 60-mg loading dose micrographs. This may explain for the decrease in particles observed from 30- to 40-mg loading. It has been hypothesised that for carrier-based formulations, when insufficient deagglomeration occurs within the device, the agglomerates impact in the USP induction port causing further detachment of API from the carrier (28).

During the aerosolisation process of the higher loading doses (*i.e.* 60-mg loading dose), the number of carrier particles within the airflow stream increases. This leads to greater number of collisions of carrier particles with the induction port leading to relatively large shard-like fragments found in the USP induction port (Fig. 3d–f).

The physical characteristics of the lactose carrier particle post-aerosolisation collected in the NGI pre-separator were analysed by SEM to establish the consequence of increasing the dose sequentially from 10 to 60 mg. It was observed that when the initial dose of formulation was 10 mg, there was efficient fine particle BDP detachment from the carrier with the majority of particles removed from the carrier surface and crevices (Fig. 4a). This efficient BDP detachment could be due to the likelihood of having higher airflow turbulence and greater individual particle momentum, resulting in larger impaction forces with other carrier particles and the dosing cup wall. Increasing the dose loading from 10 to 20 mg and 30 mg led to decreased fine particle detachment from the carrier, as noticeable amounts of BDP particles can be observed in crevices and on the surfaces of the carrier particle (Fig. 4b, c). There were significant differences in the surface morphology, with the number of BDP particles becoming more noticeable in crevices and on the smooth surface of the carrier, with subsequent increases of dose loading beyond 30 mg (Fig. 4d–f). At the greatest mass analysed (60 mg), it was observed that crevices were predominately still coated with fine particles, suggesting decreased BDP aerosolisation (Fig. 4f). As the detachment of fine particles from a carrier is influenced by forces acting on the carrier-based system, these results suggest that as the loading dose is increased, there is insufficient detachment forces (turbulence,

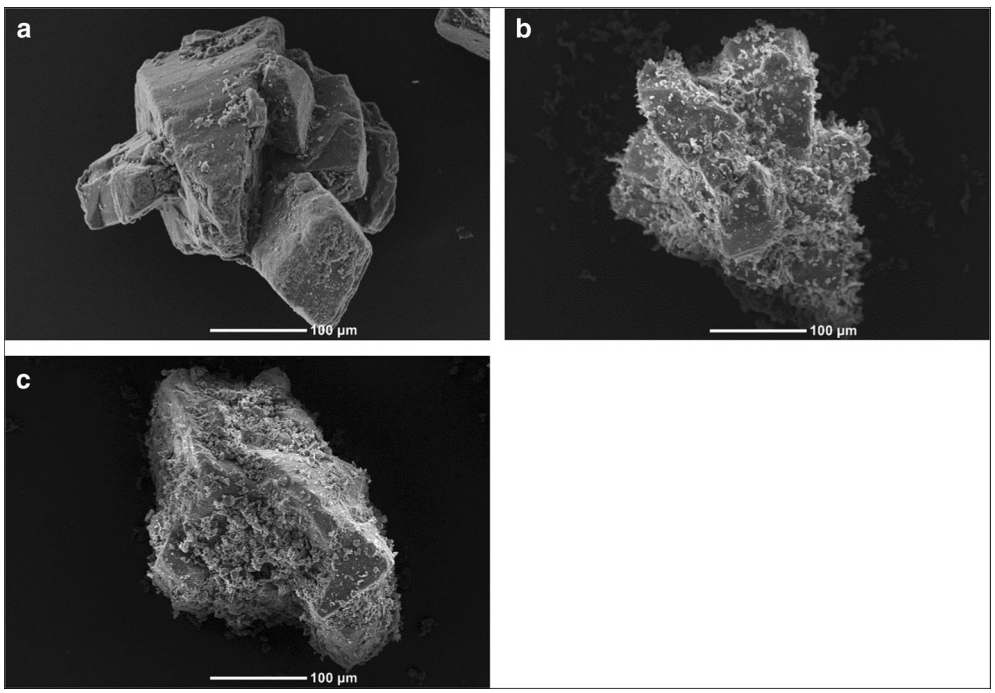

Fig. 2. Scanning electron micrographs of **a** coarse granular lactose carrier, **b** pre-blend carrier system and **c** pre-blend carrier system loaded with beclomethasone dipropionate (1% *w*/*w*)

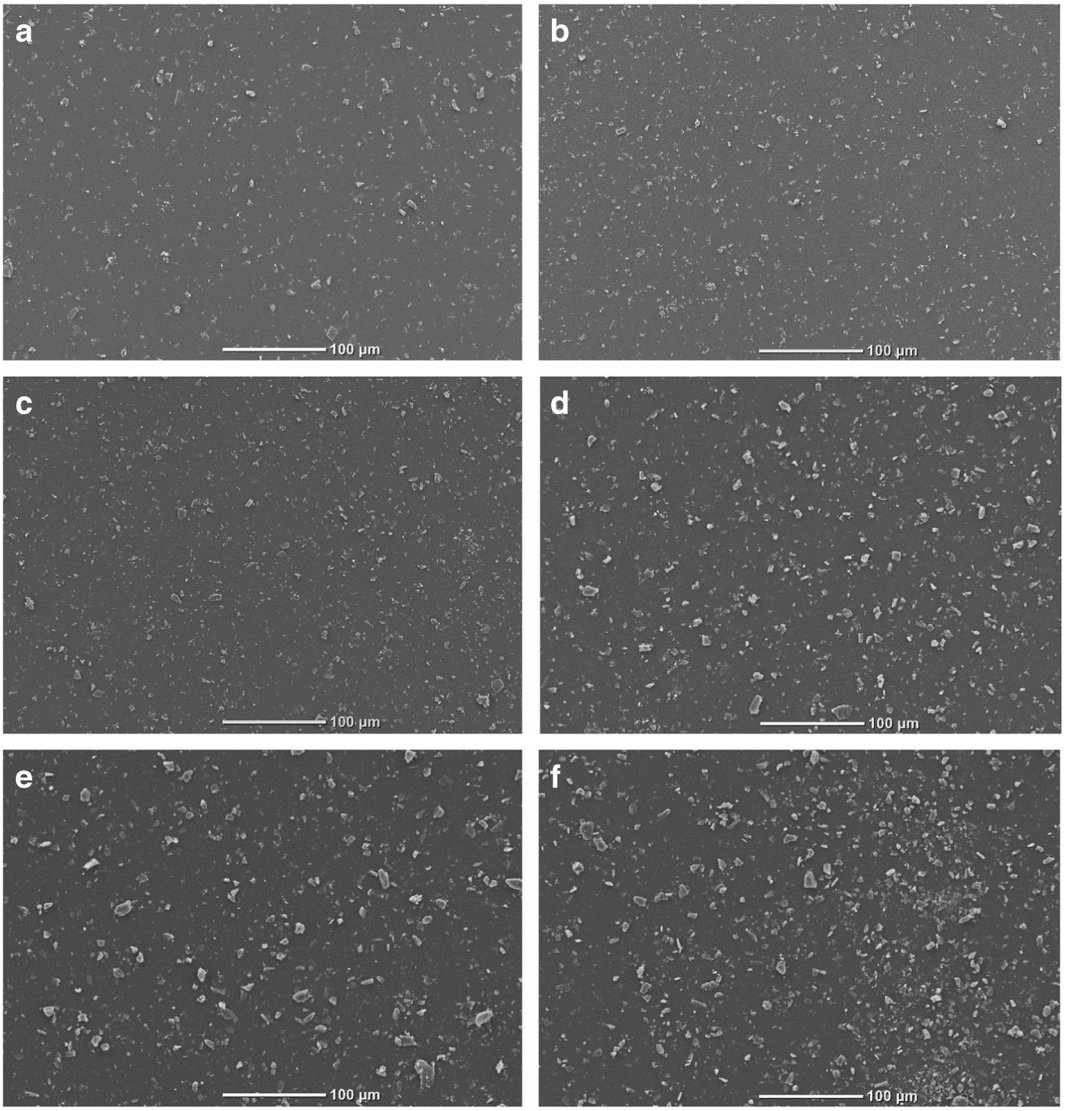

Fig. 3. Scanning electron micrographs at 240× magnification of fine particle deposition on surface of USP induction port post-aerosolisation with loading doses of **a** 10 mg, **b** 20 mg, **c** 30 mg, **d** 40 mg, **e** 50 mg and **f** 60 mg, respectively

momentum, frictional and impaction) to counteract the attachment forces (van der Waals, electrostatic, capillary and physical entrapment) (29). With sequential loading of the dosing cup, more of the cup volume is filled with dry powder formulation, leaving a reduced void space, reducing momentum and particle-particle/particle-wall impaction, therefore leading to decreased BDP detachment and inefficient aerosol dispersion of BDP from the carrier.

The decrease in BDP aerosolisation and performance is supported by micrographs of post-aerosolised fine particles found in the USP induction port and on the surface of the carrier particles in the pre-separator (Figs. 3 and 4). As increases in dose loading lead to greater BDP deposition on the surface of the USP induction port (Fig. 3), and decreased efficiency in BDP detachment with greater BDP remaining on the carrier particle (Fig. 4).

Volume of Dosing Cup Occupied by Formulation by Bulk Density

The bulk density of the formulation was found to be 0.637 ± 0.001 mg/mm^3. This was used to calculate the volume of dosing cup occupied by the different formulation mass loadings with occupied percentage between 11.8 and 70.8% (Table II) and the corresponding void volume: 88.2%, 76.4%, 64.6%, 52.8%, 41.0%, 29.2% respectively. The greater dry powder mass relative to the device geometry (in this case the dosing cup) and the resultant increased number of large carrier particles are likely to contribute to the overall adhesion/cohesion-dispersion forces (30,31). The decrease in void volume due to greater loading mass potentially leads to reduce separation distance of particle-particle and particle-wall, thus possibly causing reduction of (1) particle entrainment and dispersion, (2) turbulent forces acting upon individual particles and (3) momentum with each individual particle leading to diminished impaction forces.

Influence of Increasing Dose Loading on *In Vitro* Drug Deposition and Aerosol Performance

The *in vitro* drug deposition and aerosol performance were evaluated for each of the loading doses using the NGI. For each

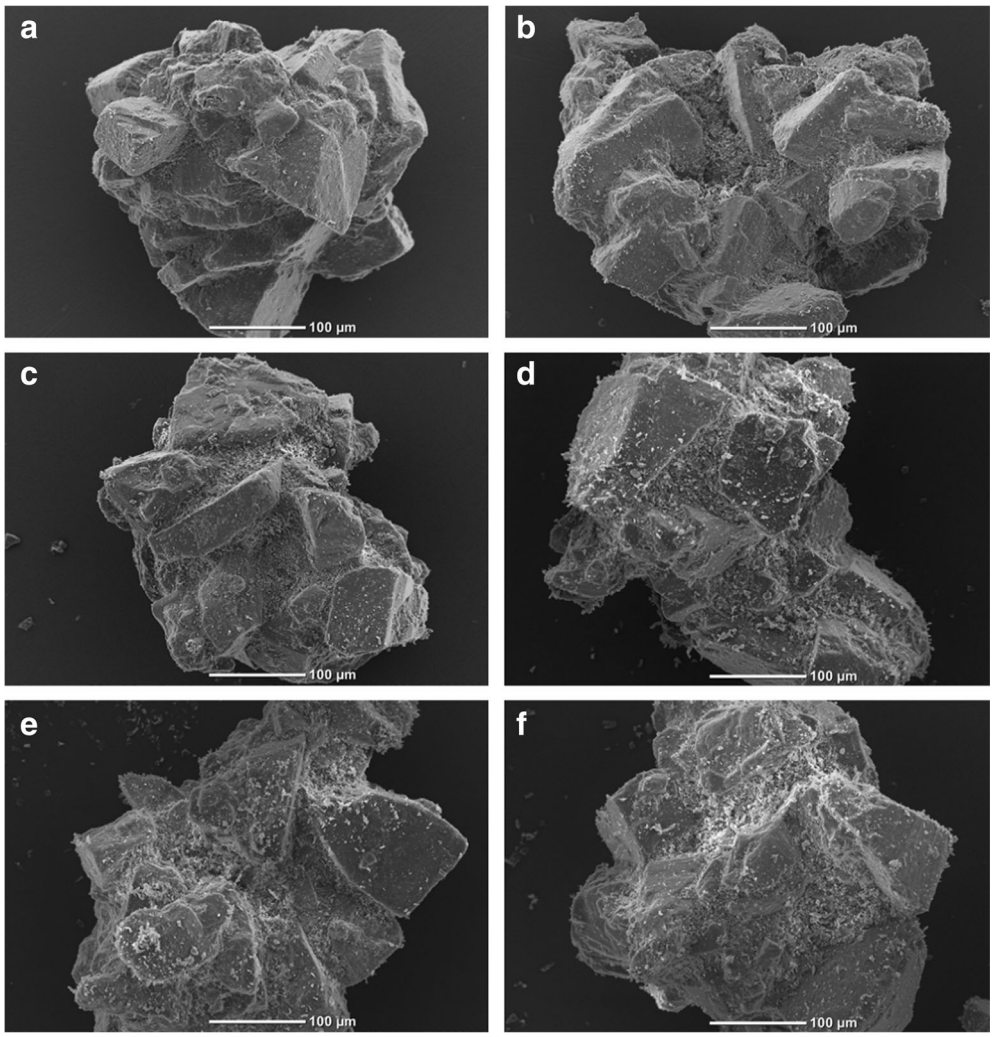

Fig. 4. Scanning electron micrographs at 240× magnification of carrier particles post-aerosolisation deposited on the NGI pre-separator of 1% BDP pre-blend carrier with loading doses of **a** 10 mg, **b** 20 mg, **c** 30 mg, **d** 40 mg, **e** 50 mg and **f** 60 mg

mass deposition investigation, the recovery from the inhaler device and each of the NGI stages, presented as the mass of BDP (µg) and the percentage of BDP compared to total mass recovered BDP, are shown in Figs. 5 a and b, respectively. By increasing the loading dose, the BDP deposition significantly increased from the pre-separator to stage 6 for each incremental loading increase (Fig. 5a). This can be also seen with other studies where it has been shown that increasing the loading dose, the amount of API delivered to the lungs can be increased (9,17).

One such study by Parumasivam et al. 2017, using a modified Aerolizer® that allowed for a larger capsule size with loading doses of up to 100 mg showed it was possible to optimise pre-existing inhalers to increase dose loading, with relatively efficient aerosol performance (8).

The modified dosing cup size enabled greater quantities of BDP to be aerosolised and delivered to the lower stages of the NGI, which translates to greater delivery of fine particle BDP to the lungs. However, evaluating the percentage of BDP deposition (Fig. 5b), there were significant amounts of BDP retained in the pre-separator with increasing dose loading, which supports the SEM observations showing decreased detachment of BDP from the carrier particles (Fig. 4). This subsequently decreases the proportion of BDP able to be delivered to the lower stages of the NGI, decreasing the efficiency of BDP deposition.

Table II. Bulk Density of 1% BDP (0.637 ± 0.001 mg/mm^3) with Corresponding Percentage of Volume Occupied in the Dosing Cup with 10 mg of Specified Formulation (Volume of 10 mg Formulation, 15.71 ± 0.03 mm^3) ($n = 3$, ± SD)

	Formulation mass loading					
	10 mg	20 mg	30 mg	40 mg	50 mg	60 mg
Cup volume 133.04 mm^3	(15.71 mm^3) 11.8%	(31.42 mm^3) 23.6%	(47.13 mm^3) 35.4%	(62.84 mm^3) 47.2%	(78.55 mm^3) 59.0%	(94.26 mm^3) 70.8%

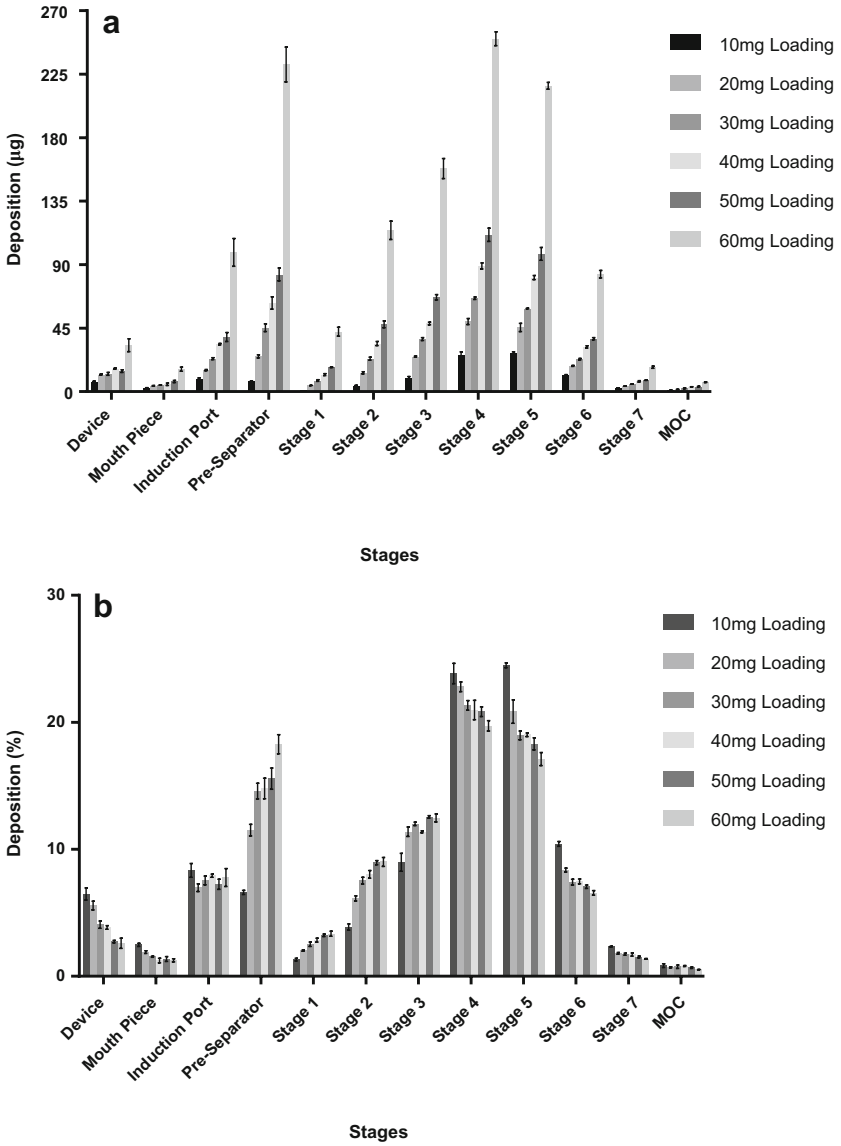

Fig. 5. Deposition of recovered BDP from the inhaler device and NGI stages with increasing loading mass with 1% BDP (*w*/*w*) formulation: **a** stage deposition mass per actuation ($n = 3$, ± SD); **b** stage deposition percentage compared to total weight of recovered BDP ($n = 3$, ± SD)

The results presented here can be considered similar to that from a current marketed high dose lactose-based carrier formulation (25 mg) DPI Relenza® utilising the Diskhaler® device (Table I). In this case, the majority of the zanamivir deposited in the pre-separator (approximately 50%), indicating that zanamivir resisted deagglomeration and/or detachment from the carrier, resulting in decreased deposition in the lower stages of the impactor (32). However, it must also be stressed that Relenza® is a high-dosed formulation (20% *w*/*w*), as opposed to the BDP (1% *w*/*w*) formulation used in this study. With high-dose concentrations other variables such as agglomeration and multi-layering can occur. These may contribute to the reduced API deagglomeration and detachment from the carrier particle and must therefore be taken into account (2).

It is also interesting to note that the percentage of BDP retained in the device decreases with increase in loading dose. There are two possible explanations for this:

1. At higher dose loading, the separation distance between particle-particle and particle-wall during aerosolisation is decreased. This leads to diminished momentum with each individual particle, reducing the impaction force of the BDP onto the cup surface, and limiting the amount of BDP adhering to the dosing cup surface (33).
2. The increased number of large carrier particles could act as 'sweeper' crystals, removing adhered BDP from the dosing cup surface (34,35). The concept of sweeper crystals was employed by de Boer et al. In this investigation, larger lactose particles (63–100, 150–200 and 250-355 μm) were added to the formulation to displace API from the inner walls of inhaler classifier chamber. This was found to reduce the API accumulation in the inhaler for high powder doses (34,35) and, in our study, theoretically increasing the FPF by making

more BDP available for dispersion. As observed, the percentage of BDP retained in the device decreased with increasing dose loading, therefore increasing the amount of BDP available for dispersion (Fig. 5b).

It can be seen with each of the mass deposition studies that increasing dose loading leads to greater amounts of fine particle BDP depositing on each of the stages in the NGI (Fig. 5a). In general, the FPD demonstrated a linear relationship (Fig. 6a) with respect to dose loading with an R^2 of 0.9966. This suggests that the FPD is very much dependent on, and predicted by, the loading dose, up to 60 mg.

Despite FPD increasing with loading dose increase, the efficiency of BDP delivery decreased. The FPF was shown to decrease significantly ($p < 0.05$) with all dose loading. Specifically, the highest FPF was found with the 10-mg dose loading, 77.0 ± 0.6%, and the lowest with 60 mg at 61.8 ± 1.3% (Fig. 6b).

Still, the FPF with loading dose of 60 mg was relative efficient, as it has been shown that commonly marketed DPIs with carrier-based formulations tend to have FPF lower than 40%, with values very much dependent on inspiratory flow rates (9,36). In a study by Buttini et al., investigating two marketed carrier-based inhaler devices, Foster® NEXThaler® with 10-mg dose loading (1.0% *w/w* of BDP) and Seretide® Diskus® with 12.5-mg dose loading (2.0% of fluticasone propionate), FPFs of 66.3 ± 3.0% and 22.9 ± 1.2% were observed, respectively (measured at 60 L/min) (20). Furthermore, two studies using Relenza® Diskhaler® (20% *w/w*) with high loading dose of 25 mg showed FPFs of 25.6 ± 2.5% and 34.2 ± 0.9%, respectively (11,32).

There was an observable difference in the rate of decrease between 10 and 30 mg and 40–60 mg (Fig. 6b). This is also supported by the MMAD, which increased with increased dose loading, possibly indicating larger sized BDP agglomerates detaching from the carrier particles or decreased efficiency in deagglomeration and fine BDP detachment from the carrier particles (Fig. 7a). Also, an increase in GSD was observed, which infers a degree of particle size variability during dispersion and therefore indicating hetero-dispersibility (Fig. 7b). However, it must also be noted that calculations are based on multiple actuations and may have contributed to the GSD for lower mass loadings emulating the decreased variability. It can also be observed that there is a direct correlation with MMAD and FPF. With increasing MMAD, there is an inversely proportional decrease in FPF (Fig. 8). It was also observed that as FPF decreases, there are two distinctive gradients (rate of decline) (Fig. 8i, ii) indicating the possibility of different forces acting on the formulation at different loading doses. Data from FPF, MMAD, GSD and particles deposited on the USP

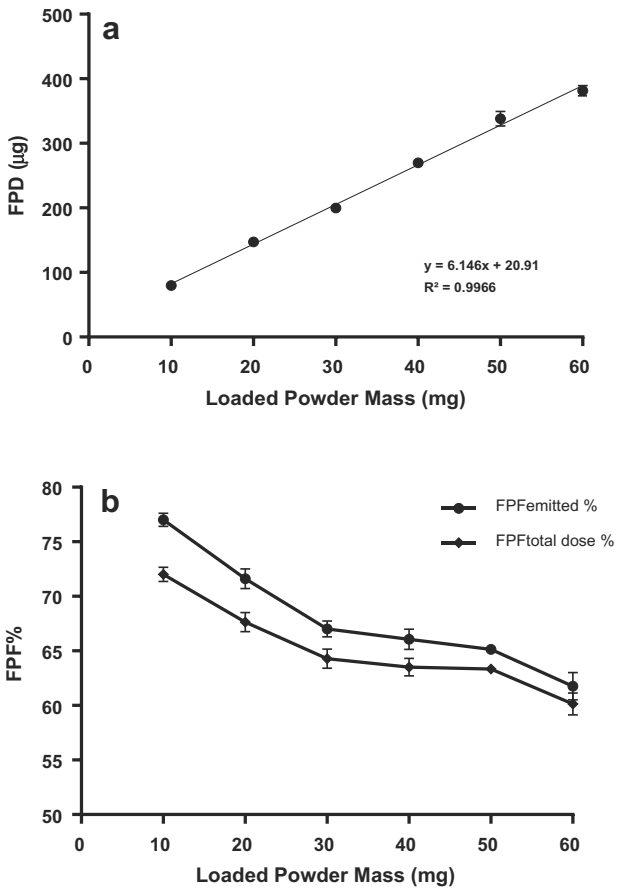

Fig. 6. Impact of increasing the loaded powder mass with 1% BDP (*w/w*) formulation on: **a** fine particle dose µg (FDP) ($n = 3$, ± SD) and **b** fine particle fraction emitted % (FPF emitted %) and fine particle fraction total dose % (FPF total dose %) ($n = 3$, ± SD)

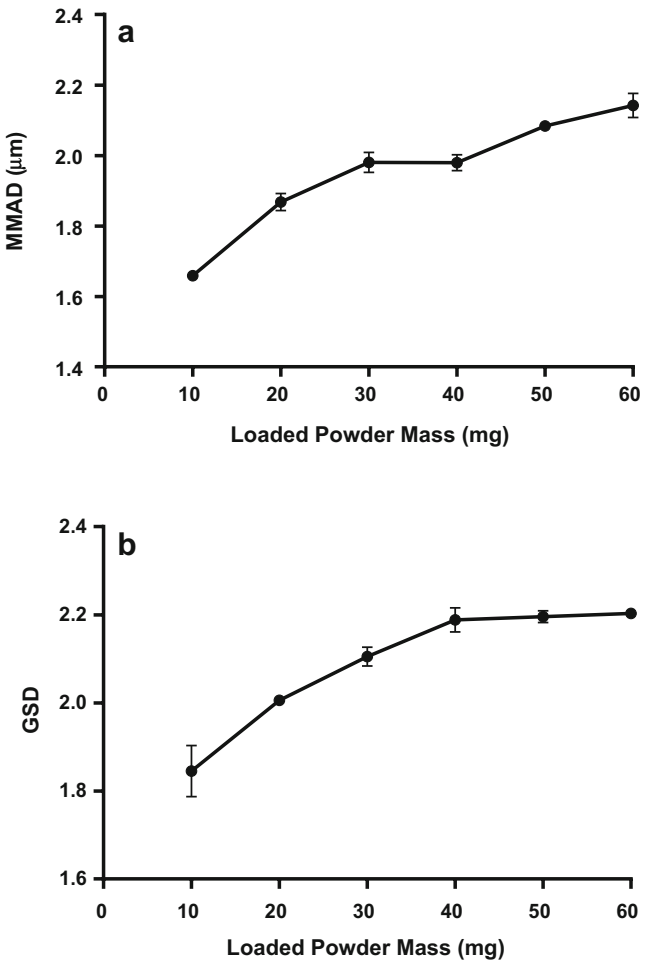

Fig. 7. Impact of increasing the loaded powder mass with 1% BDP (*w/w*) formulation on: **a** mass median aerodynamic diameter µm (MMAD) ($n = 3$, ± SD) and **b** geometric standard deviation (GSD) ($n = 3$, ± SD)

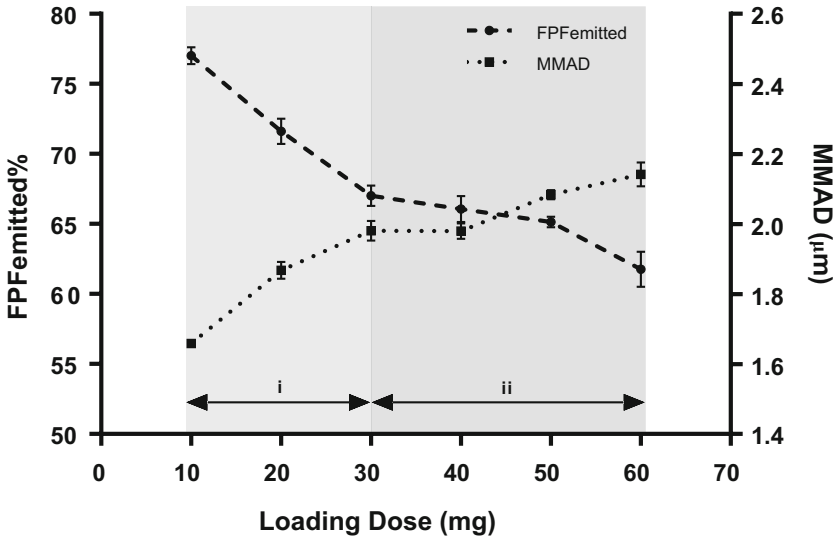

Fig. 8. Correlation between fine particle fraction emitted % (FPF emitted) ($n = 3$, ± SD) and MMAD ($n = 3$, ± SD) with theoretical aerosolisation forces: (i) decreasing impaction forces (adhesion/cohesion forces > > deagglomeration and dispersion forces) and (ii) transition where decrease in impaction forces is partially offset with lactose carrier acting as 'sweeper' particles removing BDP from inhaler surfaces (adhesion/cohesion forces > deagglomeration and dispersion forces)

induction port (visually larger in size for loading doses greater than 40 mg) suggests the possibility of a transitional point whereby the mechanistic forces involved in aerosolisation could potentially 'change' between 30 and 40 mg. This occurs as impaction forces decrease due to the reduction in void volume in the dosing cup with increasing mass loading. However, with the subsequent increase in loading mass leads to greater number of large carrier particles which acts as sweeper particles and this to some degree counteracts the reduction in impaction forces at higher mass loading doses (*i.e.* 30–60 mg).

The FPF of all dose loading in this study compares favourably with many other high load dose non-carrier formulations, using different inhaler devices (Table I). However, it must also be noted that several studies showed in Table I have employed submicron engineered particles (*i.e.* excipient enhanced growth technology) formulations, which enabled extremely improved aerosol performance even with increased loading doses (9,37).

The aerosol performance of a carrier-based DPI is determined by the conventional aerosolisation model, *i.e.* differences between adhesive/cohesive forces (physical entrapment + electrostatic forces + capillary forces + van der Waals) and deagglomeration/dispersion forces of the formulation (inertial forces + rotary forces + turbulence forces + impaction forces + shear stress) (29,38,39). The differences between the two opposing forces determine the drug delivery and the efficiency of aerosol performance. Therefore, when adhesive and cohesive forces are greater than deagglomeration and dispersion forces, there in decreased API delivery to the lungs and *vice versa*. However, this model does not explain the true complexities of the forces and other factors that may contribute to aerosolisation of a dry powder formulation with greater dose loading.

A decrease in impaction forces by sequentially increasing formulation mass leads to decreases in the void volume of the dosing cup. Since momentum = mass × velocity, $\text{velocity}_{\text{final}} = (\text{velocity}_{\text{initial}}^2 + 2 \times \text{acceleration} \times \text{distance})^{0.5}$ and $\text{velocity}_{\text{initial}} = 0$. Therefore, $\text{velocity}_{\text{final}} = (2 \times \text{acceleration} \times \text{distance})^{0.5}$ and the equations can be rewritten as follows: momentum = mass × $(2 \times \text{acceleration} \times \text{distance})^{0.5}$. With less distance between particle-particle and particle-device surface, it can be deduced that there would be a decrease in the momentum of all particles before collision with adjoining particles and with the dosing cup wall, thus leading to decreased impaction forces. Therefore, the reduction in impaction forces indicates a decrease in deagglomeration/dispersion forces leading to increasing MMAD and decreasing FPF (Fig. 8). Also, when larger masses are fit into a dosing cup with limited void space, not only inter-particular forces and tensile forces act on the particles, but also compressive forces (gravitational forces) on larger particles (> 50 μm) which leads to non-uniform forces propagating throughout the formulation known as 'force chains' (31). It was shown by Yang et al. that across the spatial distribution of packed particles, larger forces occur towards the bottom of packed fine particles and filter upwards to support the weight of the particles above the network of these packed particles (31). Unlike small particles (≤ 50 μm) where van de Waals are the dominant forces, larger particles gravitation forces are the primary inter-particle forces. Therefore, with carrier-based formulations, as with this study consisting of carrier particles in the size range of 212–355 μm (sieve fraction), compressive forces may be significant, resulting in decreased dispersion and overall aerosol performance of the formulation.

Therefore, it is essential that other forces may need to be accounted for in the aerosolisation model. The proposed model should include the addition of compressive forces (causing the presence of force chains) and the sweep forces (the displacement API from inhaler walls due to larger particles), more suitable for high dose loading carrier-based formulations in order to predict the aerosol performance.

CONCLUSION

This study has investigated the effect of increasing the loading dose of a carrier-based formulation in a reservoir-based inhaler device's dosing cup. It was demonstrated that increasing the loading dose enabled the novel dry powder inhaler with an enlarged dosing cup to deliver greater amounts of BDP, but negatively impacted on its efficiency. It also showed that the FPF was inversely correlated to the MMAD, indicating insufficient deagglomeration and/or BDP detachment from the carrier particles. In this investigation, it is also proposed that another force that is not commonly reported, contribute to the conventional aerosolisation model. This 'sweeping force' is a potential force that could be advantageous to the aerosol performance. The 'sweeping force' occurs whereby bulkier particles act like a sweeper crystal to detach adhering BDP from the walls of dosing cup, and possibly inner inhaler surfaces where the 'sweeper' particles come in contact with.

In conclusion, this study has shown that by increasing the loading dose, it is possible to increase drug delivery to the lungs, without the need for reformulation or redesigning the inhaler device. Further, investigations incorporation computational fluid dynamics coupled with discrete element method modelling would be of use in elucidating this theory.

ACKNOWLEDGEMENTS

Australian Research Council ARC LP120200744.

REFERENCES

1. Claus S, Weiler C, Schiewe J, Friess W. How can we bring high drug doses to the lung? Eur J Pharm Biopharm. 2014;86(1):1–6.
2. Yeung S, Traini D, Tweedie A, Lewis D, Church T, Young PM. Limitations of high dose carrier based formulations. Int J Pharm. 2018;544(1):141–52.
3. Schwarz C. Colobreathe® for the treatment of cystic fibrosis-associated pulmonary infections. Pulm Ther. 2015;1(1):19–30.
4. Vandevanter DR, Geller DE. Tobramycin administered by the TOBI® Podhaler® for persons with cystic fibrosis: a review. Med Devices. 2011;4:179–88.
5. Nakano T, Ishiwada N, Sumitani T, Uemori M, Isobe K, Laninamivir Prophylaxis Study G. Inhaled laninamivir octanoate as prophylaxis for influenza in children. Pediatrics. 2016;138(6).
6. Daiichi-Sankyo-Company-Limited. Inavir-Instructions of use 2018:2.
7. Begat P, Morton DAV, Staniforth JN, Price R. The cohesive-adhesive balances in dry powder inhaler formulations I: direct quantification by atomic force microscopy. Pharm Res. 2004;21(9):1591–7.
8. Parumasivam T, Leung SS, Tang P, Mauro C, Britton W, Chan HK. The delivery of high-dose dry powder antibiotics by a low-cost generic inhaler. AAPS J. 2017;19(1):191–202.
9. Farkas DR, Hindle M, Longest PW. Characterization of a new high-dose dry powder inhaler (DPI) based on a fluidized bed design. Ann Biomed Eng. 2015;43(11):2804–15.
10. Hoppentocht M, Akkerman OW, Hagedoorn P, Frijlink HW, de Boer AH. The Cyclops for pulmonary delivery of aminoglycosides; a new member of the Twincer family. Eur J Pharm Biopharm 2015;90:8–15.
11. Yang Y, Yang Z, Ren Y, Mei X. Effects of formulation and operating variables on zanamivir dry powder inhalation characteristics and aerosolization performance. Drug Deliv. 2014;21(6):480–6.
12. Young PM, Crapper J, Philips G, Sharma K, Chan HK, Traini D. Overcoming dose limitations using the orbital® multi-breath dry powder inhaler. J Aerosol Med pulmonary Drug Deliv. 2014;27(2):138–47.
13. Zhu B, Padroni M, Colombo G, Phillips G, Crapper J, Young PM, et al. The development of a single-use, capsule-free multi-breath tobramycin dry powder inhaler for the treatment of cystic fibrosis. Int J Pharm. 2016;514(2):392–8.
14. Maltz DS, Paboojian J. Device engineering insights into TOBI Podhaler: a development case study of high efficiency powder delivery to cystic fibrosis patients. Respir Drug Deliv. 2011;1:55–66.
15. Schuster A, Haliburn C, Doring G, Goldman MH, Freedom Study G. Safety, efficacy and convenience of colistimethate sodium dry powder for inhalation (Colobreathe DPI) in patients with cystic fibrosis: a randomised study. Thorax. 2013;68(4):344–50.
16. Hagedoorn P, Grasmeijer F, Hoppentocht M, Akkerman O, Frijlink H, De Boer A. *In vitro* evaluation of the Twincer colistin dry powder inhaler as a non-cough-inducing alternative to Colobreathe. Eur Respir J. 2016;48(Suppl 60):PA2561.
17. Fernandes JV, deAndrade GR, Villax P. Scaling up for high dose delivery to the lungs. ONdrugDelivery. 2016;(72):30–3.
18. de Boer AH, Hagedoorn P, Woolhouse R, Wynn E. Computational fluid dynamics (CFD) assisted performance evaluation of the Twincer disposable high-dose dry powder inhaler. J Pharm Pharmacol. 2012;64(9):1316–25.
19. GlaxoSmithKline. Highlights of prescribing information - Incruse® Ellipta®. 2016.
20. Buttini F, Brambilla G, Copelli D, Sisti V, Balducci AG, Bettini R, et al. Effect of flow rate on in vitro aerodynamic performance of NEXThaler in comparison with Diskus and Turbohaler dry powder inhalers. J Aerosol Med Pulm Drug Deliv. 2015;28:1–12.
21. Corradi M, Chrystyn H, Cosio BG, Pirozynski M, Loukides S, Louis R, et al. NEXThaler, an innovative dry powder inhaler delivering an extrafine fixed combination of beclometasone and formoterol to treat large and small airways in asthma. Expert Opin Drug Deliv. 2014;11(9):1497–506.
22. British Pharmacopoeia Commision. British Pharmacopoeia Volume V Appendix XII C. Consistency of Formulated Preparations 3. Uniformity of Content. London: TSO; 2017.
23. British Pharmacopoeia Commision. British Pharmacopoeia Volume V Appendix XII C. Consistency of Formulated Preparations 7. Preparations for Inhalation: Aerodynamic Assessment of Fine Particles. London: TSO; 2017.
24. Shalash AO, Elsayed MMA. A new role of fine excipient materials in carrier-based dry powder inhalation mixtures: effect on deagglomeration of drug particles during mixing revealed. AAPS PharmSciTech. 2017;18(8):2862–70.
25. Young PM, Edge S, Traini D, Jones MD, Price R, El-Sabawi D, et al. The influence of dose on the performance of dry powder inhalation systems. Int J Pharm. 2005;296(1–2):26–33.
26. Grasmeijer F, Lexmond AJ, van den Noort M, Hagedoorn P, Hickey AJ, Frijlink HW, et al. New mechanisms to explain the effects of added lactose fines on the dispersion performance of adhesive mixtures for inhalation. PLoS One. 2014;9(1):e87825.
27. de Boer AH, Dickhoff BH, Hagedoorn P, Gjaltema D, Goede J, Lambregts D, et al. A critical evaluation of the relevant parameters for drug redispersion from adhesive mixtures during inhalation. Int J Pharm. 2005;294(1–2):173–84.
28. Tang P, Kwok PC, Tong Z, Yang R, Raper JA, Chan HK. Does the United States Pharmacopeia throat introduce de-agglomeration of carrier-free powder from inhalers? Pharm Res. 2012;29(7):1797–807.
29. Peng T, Lin S, Niu B, Wang X, Huang Y, Zhang X, et al. Influence of physical properties of carrier on the performance of dry powder inhalers. Acta Pharm Sin B. 2016;6(4):308–18.
30. Yang RY, Zou RP, Yu AB. Computer simulation of the packing of fine particles. Phys Rev E Stat Phys Plasmas Fluids Relat Interdiscip Topics. 2000;62(3 pt B):3900–8.
31. Yang RY, Zou RP, Yu AB, Choi SK. Characterization of interparticle forces in the packing of cohesive fine particles. Phys Rev E Stat Nonlinear Soft Matter Phys. 2008;78(3 Pt 1):031302.

32. Garcia A, Mack P, Williams S, Fromen C, Shen T, Tully J, et al. Microfabricated engineered particle systems for respiratory drug delivery and other pharmaceutical applications. J Drug Deliv. 2012;2012:941243.
33. Ariane M, Sommerfeld M, Alexiadis A. Wall collision and drug-carrier detachment in dry powder inhalers: using DEM to devise a sub-scale model for CFD calculations. Powder Technol. 2018;334:65–75.
34. de Boer AH, Hagedoorn P, Gjaltema D, Goede J, Frijlink H. Air classifier technology (ACT) in dry powder inhalationPart 1. Introduction of a novel force distribution concept (FDC) explaining the performance of a basic air classifier on adhesive mixtures. Int J Pharm. 2003;260(2):187–200.
35. de Boer AH, Hagedoorn P, Westerman EM, Le Brun PP, Heijerman HG, Frijlink HW. Design and in vitro performance testing of multiple air classifier technology in a new disposable inhaler concept (Twincer) for high powder doses. Eur J Pharm Sci. 2006;28(3):171–8.
36. Demoly P, Hagedoorn P, de Boer AH, Frijlink HW. The clinical relevance of dry powder inhaler performance for drug delivery. Respir Med. 2014;108(8):1195–203.
37. Behara SR, Farkas DR, Hindle M, Longest PW. Development of a high efficiency dry powder inhaler: effects of capsule chamber design and inhaler surface modifications. Pharm Res. 2014;31(2):360–72.
38. Capece M, Silva KR, Sunkara D, Strong J, Gao P. On the relationship of inter-particle cohesiveness and bulk powder behavior: Flowability of pharmaceutical powders. Int J Pharm. 2016;511(1):178–89.
39. Weiler C, Wolkenhauer M, Trunk M, Langguth P. New model describing the total dispersion of dry powder agglomerates. Powder Technol. 2010;203(2):248–53.